Journal of Sound and Vibration 326 (2009) 353–366

Contents lists available at ScienceDirect

Journal of Sound and Vibration

journal homepage: www.elsevier.com/locate/jsvi

A generalized dynamic balancing procedure for the AH-64 tail rotor ☆

Donald L. Kunz *,[1], Mark C. Newkirk [2]

Air Force Institute of Technology, Wright-Patterson AFB, OH, USA

ARTICLE INFO

Article history:
Received 13 May 2008
Received in revised form
25 February 2009
Accepted 22 April 2009
Handling Editor: C.L. Morfey
Available online 30 May 2009

ABSTRACT

The tail rotors on the AH-64A Apache and AH-64D Longbow Apache incorporate a unique design, which includes two, two-bladed teetering rotors that have an azimuth spacing of 55°, instead of the more usual 90°. Maintainers have observed that some Apache tail rotors can be extraordinarily difficult to balance dynamically. This investigation uses RCAS (Rotorcraft Comprehensive Analysis System) numerical simulations of tail rotor response when mass is added to the tips of single and adjacent blades to investigate possible causes for this balancing difficulty. The simulations show that the 1/rev, vertical, vibratory force response due to added tip mass varies as a function of the mass distribution between two adjacent blades, and the azimuth spacing between the two blades. As a result, the tail rotor balance sensitivity coefficients, if used as for a single blade, will be inaccurate; and may be a prime contributor to the problems observed while balancing tail rotors. An analytical model of the AH-64D tail rotor, with characteristics similar to the RCAS model, and which incorporates the influence of structural impedance through the balance sensitivity coefficients and phase angles, is used to develop a method for accurately determining the amount of tip mass required to reduce the 1/rev vibrations to acceptable levels.

Published by Elsevier Ltd.

1. Introduction

The Army's AH-64A Apache was first designed by the former Hughes Aircraft Toolco Aircraft Division in response to a 1972 Department of Defense Request For Proposal (RFP) for an Advanced Attack Helicopter. In September 1975, the prototype YAH-64 made its first flight. Since 1975, the Apache contract has been executed under four different company names, and currently the program is owned by Boeing. The US Government has purchased 827 AH-64A Apache aircraft, of which 530 will be remanufactured to become the AH-64D Longbow Apache. Tests have demonstrated that the Longbow Apache is 400 percent more lethal (hitting more targets), 720 percent more survivable, and requires one-third fewer maintenance hours per flight hour than the AH-64A [1]. In the past 23 years, the Apache has played an integral role in numerous world events, including Operation Restore Hope in Somalia, Operation Desert Storm, peacekeeping in Bosnia, and most recently in the Global War on Terror.

☆ The views expressed in this article are those of the authors and do not reflect the official policy or position of the United States Air Force, United States Navy, Department of Defense, or the US Government.

* Corresponding author. Tel.: +1 937 255 3636 × 4548; fax: +1 937 656 7053.
E-mail address: donald.kunz@afit.edu (D.L. Kunz).
[1] Associate Professor, Department of Aeronautics and Astronautics.
[2] Lieutenant Commander, United States Navy.

0022-460X/$ - see front matter Published by Elsevier Ltd.
doi:10.1016/j.jsv.2009.04.043

Fig. 1. AH-64 Apache tail rotor hub and rotor blades.

Although many improvements and technological advances have been incorporated in the AH-64D, the tail rotor remained unchanged. The Apache tail rotor is unusual in two respects. First, unlike other four-bladed tail rotors (e.g., the SH-60 Seahawk), the Apache tail rotor consists of two teetering, two-bladed rotors, rather than a single four-bladed rotor. Second, while the blades on other four-bladed tail rotors are equally spaced azimuthally, the inner rotor on the AH-64 is rotated only 55° opposite the direction of rotation (see Fig. 1). The original reason for this unusual azimuth offset was to allow sufficient clearance for the pitch links, which were located such that the teetering hinge had a delta-three angle of 35°, which allows the blades to simultaneously flap and feather. Subsequently, during test and evaluation of the aircraft, it was discovered that this configuration also reduces the tail rotor noise, as compared to the conventional configuration.

Specific maintenance actions on an aircraft require it to complete a maintenance test flight (MTF). A test flight determines the proper functions of all the helicopter's systems. The systems checked include engine performance, stability and control, avionics, and vibration analysis. A typical helicopter can spend approximately 8 percent of its lifetime hours on maintenance test flights [2]; and that only accounts for the time airborne, and does not account for the time spent on the ground with the engines running. Since only the actual "flight" hours of an aircraft are recorded, it is impossible to accurately determine the total amount of time spent performing the ground procedures of an MTF. Based on the experience of the second author, it is estimated that approximately half again the time spent on a maintenance test flight is spent on the ground performing such functions as verifying the functionality of the avionics systems and performing track and balance for the main rotor and balancing the tail rotor.

The US Army Aviation and Missile Research Development and Engineering Center (AMRDEC) has observed that on numerous occasions, individual Apache tail rotors cannot be balanced using established methods for tail rotor balancing. Current balancing methods approximate the rotor system as a conventional 4-bladed rotor, with all blades rotating in the same plane, but use different sensitivity coefficients for the inner and outer rotors. Given the unusual configuration of the Apache tail rotor, it is not completely unexpected that using conventional balance techniques would occasionally produce inaccurate results, since those techniques assume that the rotor has a conventional four-bladed configuration. When the tail rotor is not adequately balanced, large, in-plane, 1/rev vibrations may be experienced at the rotor hub.

Helicopter rotor track and balance or rotor smoothing, while not a topic of intense research, has received significant attention over the past 10–15 years. Rosen and Ben-Ari created a mathematical model of a helicopter rotor that could be used to analyze rotor smoothing methodologies [3], and subsequently showed that merely forcing all of the blades to fly in the same track may not minimize out-of-plane, 1/rev vibrations [4]. Additional research has concentrated on improving the algorithms used to convert raw vibrations measurements into corrective adjustments. The methodology underlying many, or perhaps most, rotor smoothing implementations assumes that the mapping between vibrations and adjustments is linear, although corrections that account for statistical [5] or probabilistic [6] variations are often included. However, it has also been suggested that the linear assumption is overly simplistic; and that more sophisticated algorithms, which can account for nonlinearities, should be implemented [7]. Several algorithms, including neural networks [7–11], fuzzy logic [12], and interval modeling [13] have been investigated.

In the majority of the citations above, the primary concern of the research was eliminating the out-of-plane, 1/rev vibrations, which primarily result from aerodynamic dissimilarities among the rotor blades. There is very little discussion of the balancing aspect of rotor smoothing, which involves equalizing the inertia imbalance among the blades, and results in 1/rev vibrations in the plane of the rotor. This investigation will focus specifically on dynamic balancing of helicopter tail rotors, but the methodology may be generalized to the main rotor as well. First, this investigation will identify possible causes for the observation that some Apache tail rotors are difficult to balance. Then, it will look into means for improving tail rotor balancing methods, without having to institute major changes in existing methods.

2. Apache tail rotor

The Apache tail rotor consists of two, two-bladed rotor hubs. Each hub is teetering and semi-rigid, with a delta-three angle of 35° [14]. The inner and the outer hubs are located 30.6 and 36.5 in from the fuselage centerline, respectively, on the port side of the aircraft. The blades on the inner and outer rotors are offset by an angle of 55°, with the inner rotor blades trailing the outer blades. As a result, inboard blade 1 trails outboard blade 1 by 55°, and inboard blade 2 also trails outboard blade 2 by 55° (see Fig. 2). Similarly, The angle between outboard blade 2 trails inboard blade 1 by 125°, and outboard blade 1 trails inboard blade 2 by the same angle.

The only control input to the tail rotor is collective pitch. The pilot controls collective pitch with the foot pedals. A cable mechanism transfers the pilot input to the tail rotor pitch control mechanism, which is connected to the blades by pitch bearings and pitch links which in turn transfer the pilot inputs to the blades via the swashplate. When both pedals are centered (50 percent pedal input), the blades on the AH-64 have a built-in collective pitch angle of 7.4°.

2.1. Tail rotor balancing

Unlike the main rotor system, where the rotor blades are both tracked and balanced to minimize 1/rev vibrations, the tail rotor blades are balanced, but not tracked. For both the main and tail rotors, balance procedures are performed while the aircraft is parked on the ground. Early balance methods only consisted of static mass balancing of the rotor, in order to minimize in-plane, 1/rev vibrations by making the mass distribution as symmetrical as possible. However dynamic effects also play a role in rotor imbalance. Current methods of balancing tail rotors on most helicopters (including the Apache tail rotor) involve performing a static balance and adding and removing weights from individual blades to achieve dynamic balance. On the Apache tail rotor blades, there are two pockets on the blade tip where the adjustment weights are attached. During the balancing procedure, weights are equally split between the pockets, with half the weight adjustment made to the forward pocket and half the weight adjustment made to the aft pocket. This maintains chordwise balance of the blade.

The instrumentation used during the balancing procedure includes an accelerometer attached to the vertical tail (Fig. 2), and an optical tachometer. The accelerometer measures the vertical vibratory accelerations imparted to the tail by the in-plane vibrations of the tail rotor hub. The optical tachometer provides an accurate reading of the tail rotor angular velocity,

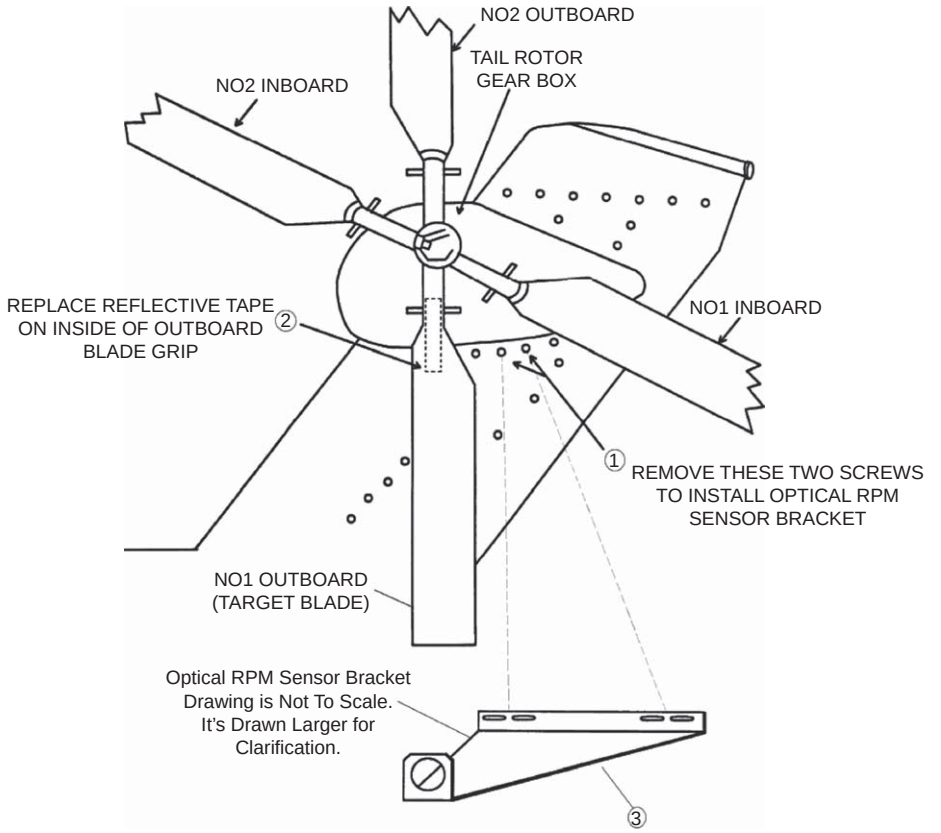

Fig. 2. Apache tail rotor schematic [16].

using outboard blade 1 as the target blade. Approximately 40–50 revolutions of data are collected from the tail rotor accelerometer and tachometer for each test run.

The acceleration and tachometer data from each test run is collected by either the Aviation Vibration Analyzer (AVA) or the Vibration Management Enhancement Program (VMEP). AVA uses a linear algorithm to calculate the amount of weight that must be added or subtracted from the blade tip weight pockets in order to minimize the 1/rev vibratory accelerations; while VMEP uses neural networks [15]. The algorithm used by AVA is based on sensitivity coefficients that have been derived by the least squares method from an empirical database of vibratory responses to known weight adjustments. VMEP's neural networks are also trained using an empirical database of vibratory responses to known weight adjustments. Although AVA and VMEP employ different algorithms to calculate a balance adjustment solution from accelerometer and tachometer data, the relationship between the adjustment solution and a particular vibration amplitude and phase angle is linear [15]. In practice, the balance coefficients are only about 80 percent accurate, due to factors such as electronic noise, weather, and differences in individual airframes of the same aircraft type.

2.2. RCAS tail rotor model

A tail rotor simulation used to calculate the vibratory response of Apache tail rotor system was implemented using the Rotorcraft Comprehensive Analysis System (RCAS), an advanced computational analysis program for rotorcraft. RCAS was developed by both the US Army Aeroflightdynamics Directorate (AFDD) and Advanced Rotorcraft Technology, Inc. (ART) to establish a standard analysis tool for the helicopter community to use for research, engineering, and design of helicopters. The program has assisted in improving helicopters that are currently in production along with providing a comprehensive analysis of structural dynamics, aeroelastic stability, vibration, stability and control, performance and loads, and flight dynamics before a prototype is created. For the purposes of this investigation, the tail rotor simulation was used to characterize the vibratory loads produced by an unbalanced tail rotor.

The Apache tail rotor is modeled in RCAS as two, completely separate, two-bladed, coaxial, teetering rotors. The geometry and kinematics of the rotors are faithfully modeled, except that the delta-three angle is not included. The tail rotor is designed with a delta-three angle in order to minimize the teetering of tail rotor blades. When the rotor teeters, the positive delta-three angle decreases the pitch angle of the higher blade and increases the pitch angle of the lower blade. As a result, the rotor tends to return to zero teetering angle. Since balancing is performed with the tail rotor stationary, and there is no cyclic pitch control on the tail rotor, the rotors would not be expected to teeter. The blades are assumed to be rigid, and are modeled using the RCAS Rigid Blade element. A Rigid Body Mass element is attached at the tip of each blade to model the blade imbalance. When the rotor is in balance, the tip masses are set to zero mass. In order to create an imbalance, the tip masses on each blade can be set to nonzero values individually.

Aerodynamic modeling of the blades includes the built-in twist of the blades and the 7.4° collective pitch angle when the pedals are centered. The forces and moments produced by the NACA 63414-mod airfoil are represented by airfoil tables. A uniform inflow model is used as well as a tip loss factor of 0.95. All of the blades were modeled to be aerodynamically identical. While aerodynamic dissimilarities among the blades could result in differences in profile and induced drag on the blades, the effect on 1/rev, in-plane vibrations is expected to be small compared to the impact of mass imbalance. Furthermore, since tail rotors in general, and the Apache tail rotor in particular, have no mechanism (such as trim tabs) to adjust for aerodynamic dissimilarities, mass balancing would not be an effective method for eliminating 1/rev, in-plane vibrations due to aerodynamic dissimilarities. After running many simulations with the rotor both balanced and unbalanced, it was confirmed that the effect of the aerodynamic forces on the 1/rev, in-plane, vibratory response was not significant.

3. Simulation results and discussion

The methodology used to investigate the difficulties in balancing certain Apache tail rotors consisted of running trimmed tail rotor simulations with the RCAS tail rotor model. Weights were added to the tips of individual blades, and the forces at the hub of the tail rotor were calculated. Since force is proportional to acceleration, force comparisons for various tip weight cases are equivalent to acceleration comparisons. In keeping with the convention specified in [16], outboard blade 1 was used as the reference blade. In the results to follow, the force response amplitude is defined as the half peak-to-peak amplitude; and the phase angle is defined as the azimuth angle where the force response passes through the mean value of the response from below.

3.1. Tip mass added to a single blade

In the first series of simulations, tip masses were added to individual blades, one at a time. This methodology is equivalent to the procedure used to derive the empirical balance coefficients from flight tests. First, increasing masses were added to outboard blade 1. Fig. 3 shows the vertical force response at the rotor hub as a function of azimuth for each tip mass. As expected, the amplitude of the vertical force response increases as the tip mass increases, and the phase

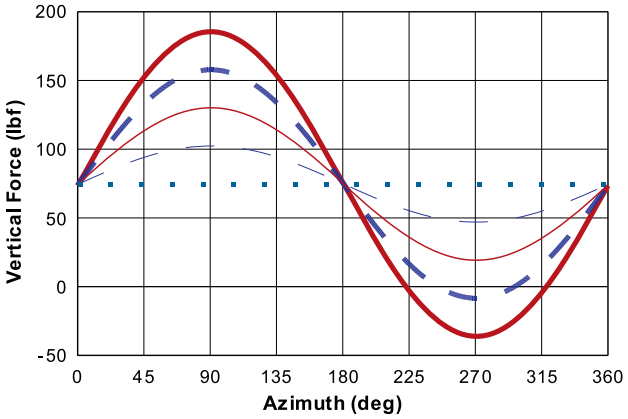

Fig. 3. Vertical force response for outboard blade 1. ····· 0 g, - - - - 4 g, —— 8 g, ▬ ▬ 12 g, ▬▬ 16 g.

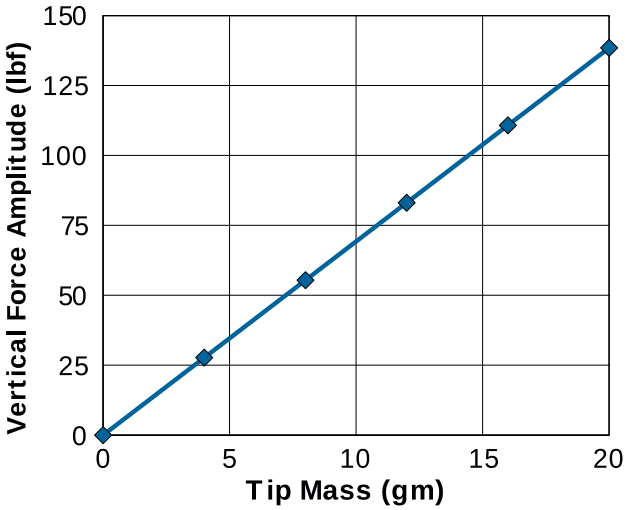

Fig. 4. Vertical force amplitude versus tip mass for outboard blade 1.

relationship remains constant. It should also be noted that the 74.65 lbf mean value of the vertical force response represents static load due to the mass of the tail rotor blades.

The vertical force response amplitudes are plotted against the tip mass in Fig. 4, which clearly shows that the relationship between the tip mass and the response amplitude is linear. This result is consistent with flight test data used to derive the balance sensitivity coefficients. Fig. 3 also shows that the azimuth angle where the response crosses the mean value from below is approximately 0° (0.61°, to be exact). Since outboard blade 1 is the reference blade, this angle is an excellent choice to represent the phase angle of the vibratory response. To determine the phase angles for the vibratory response of each of the other blades, 10 g masses were sequentially attached to each of the tail rotor blades, and the vertical force responses were calculated. The results in Fig. 5 show that the phase angle of the vertical force response corresponds to the geometric configuration of the tail rotor (see Fig. 2). That is, the response phase angle for inboard blade 1 is 55°, the response phase angle of outboard blade 2 is 180°, and the response phase angle of inboard blade 2 is 235°.

To demonstrate how these results may be used for rotor balance, first consider the linear relationship shown in Fig. 4. The slope of the curve is the inverse of the balance sensitivity coefficient which has a value of 6.9217 lbf/g. Now, suppose that an unknown tip mass is added to one of the blades in the model, and the resulting vibratory force has an amplitude of 40 lbf and a phase angle of 235°. Based on Fig. 5, the phase angle predicts that the mass must have been added to inboard blade 2; and from the sensitivity coefficient, the amount of mass added was 5.78 g. In order to balance the rotor and eliminate the 1/rev vibration, 5.78 g must be removed from inboard blade 2. Since the tip weights are normally added (or removed) in 2 g increments, 6 g would be removed from inboard blade 2 in order to minimize the 1/rev vibration due to the mass imbalance. This methodology is typical of algorithms used in the vibration analysis equipment that is used to balance helicopter tail rotors.

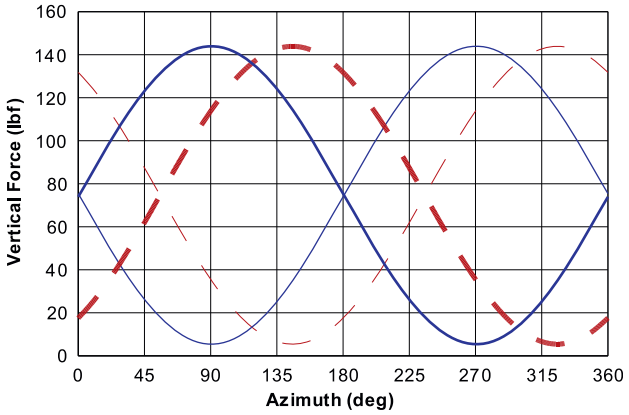

Fig. 5. Vertical force response for 10 g tip masses added to individual blades. ▬▬ outboard blade 1, —— outboard blade 2, ▬ ▬ ▬ inboard blade 1, – – – – inboard blade 2.

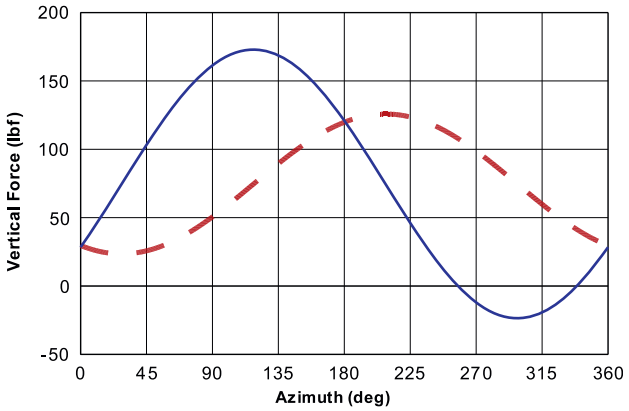

Fig. 6. Vertical force response from 8 g on outboard blade 1 and inboard blade 1 (▬▬), and on inboard blade 1 and outboard blade 2 (▬ ▬ ▬).

The results presented above clearly show that when tip masses are added to a single tail rotor blade, the amplitude of the vertical response varies linearly with the amount of mass; and the phase angle is an accurate predictor of the blade to which the mass was added. Therefore, when a single tail rotor blade is out of balance, the methodology and procedures currently in use should be sufficient to accurately balance the tail rotor.

3.2. *Tip masses added to adjacent blades*

Prediction of the amount of tip mass from the amplitude and phase of the vibratory force becomes significantly more complicated when tip masses are added to adjacent blades. Fig. 6 shows two cases: one is the vertical vibratory response when 8 g are added to outboard blade 1 and 8 g are added to inboard blade 1 (solid line); and the other is the vertical vibratory response when 8 g are added to inboard blade 1 and 8 g are added to outboard blade 2 (dashed line). In both cases, the phase angles can be used to accurately determine the proportion of mass that was added to each blade. That is, in the first case, the phase angle is 28.11°, which is approximately equal to 27.50°, the azimuth angle half way between outboard blade 1 and inboard blade 1; and the phase angle in the second case is 118.11°, which is approximately equal to 117.50°, the azimuth angle half way between inboard blade 1 and outboard blade 2. However, the balance sensitivity coefficient of 6.9217 lbf/g from Fig. 4 incorrectly predicts that the total amount of mass added to the two blades in the first case was 14.19 g, and the total mass added to the two blades in the second case was only 7.39 g. The variation in the vertical response amplitude for certain mass distributions, but the same total mass, becomes even more confusing if one looks at the vertical force response for the full range of mass distributions. Fig. 7 shows the vertical response amplitude versus phase angle for a total of 16 g, distributed between two adjacent blades. At the far left of the figure, all 16 g are on outboard blade 1. For the next point to right, 2 g are shifted to inboard blade 1; and for each succeeding point, two additional grams are shifted, until all 16 g are on inboard blade 1. The same pattern is repeated, shifting mass in 2 g increments from inboard blade 1 to outboard blade 2; then from outboard blade 2 to inboard blade 2; and finally from inboard blade 2 back to

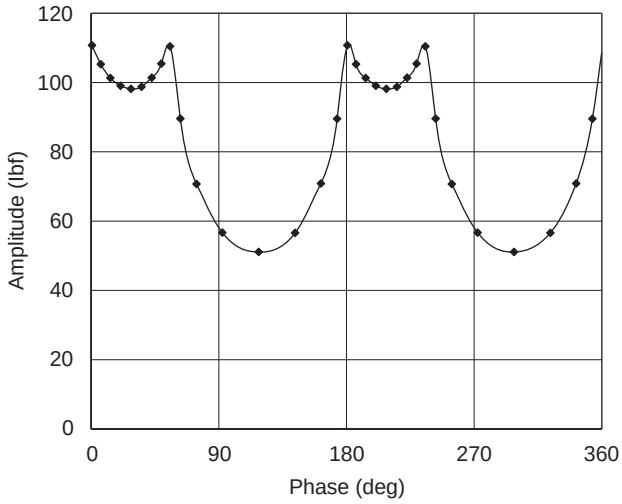

Fig. 7. Vertical response amplitude versus phase angle for 16 g total mass.

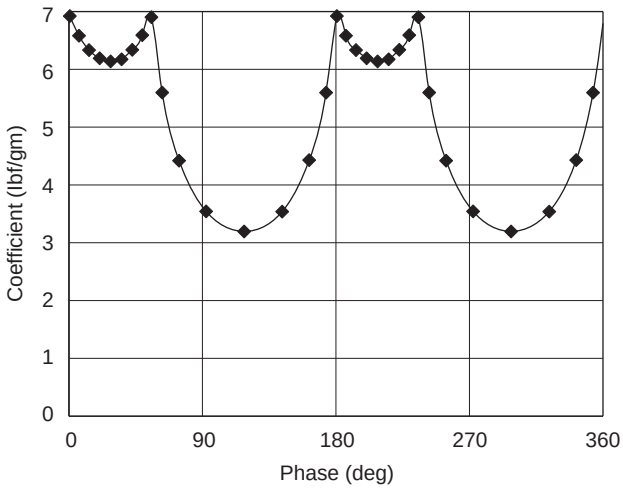

Fig. 8. Balance sensitivity coefficients versus phase angle.

outboard blade 1. This figure clearly shows that not only does the vertical force response depend on the mass distribution between the two blades, but it also depends on the azimuth spacing of the two blades.

The vertical force response shown in Fig. 7 can also be transformed into balance sensitivity coefficients, as shown in Fig. 8. When all of the mass is concentrated on one blade (0°, 55°, 180°, 235°), the sensitivity coefficient is equal to the value found in Fig. 4. It can also be seen from this figure that the sensitivity coefficient varies with the mass distribution, as indicated by the phase angle. For two adjacent blades, the sensitivity coefficient is a minimum when the mass is distributed equally between them. In addition, it is apparent that blade azimuth spacing is the primary factor controlling the magnitude of the difference between the minimum and maximum coefficients for mass distributed between two adjacent blades.

It is significant to note that since blade azimuth spacing is the reason why the vertical response amplitude and the sensitivity coefficients exhibit the behavior shown in Figs. 7 and 8, respectively, other configurations will exhibit different behavior. For example, the tail rotor design for the Mil MI-28 Havoc is similar to that of the AH-64, but the spacing between the two teetering rotors is 35°. Therefore, one would expect the magnitude of the difference between the maximum and minimum coefficients to be smaller for the blades spaced 35° apart, and larger for the blades spaced 145° apart (compared to Fig. 8). More significantly, for the conventional configuration where the azimuth spacing between all adjacent blades is 90°, the difference between the maximum and minimum coefficients would be equal for all adjacent blades, and somewhere between the minimum values shown in Fig. 8.

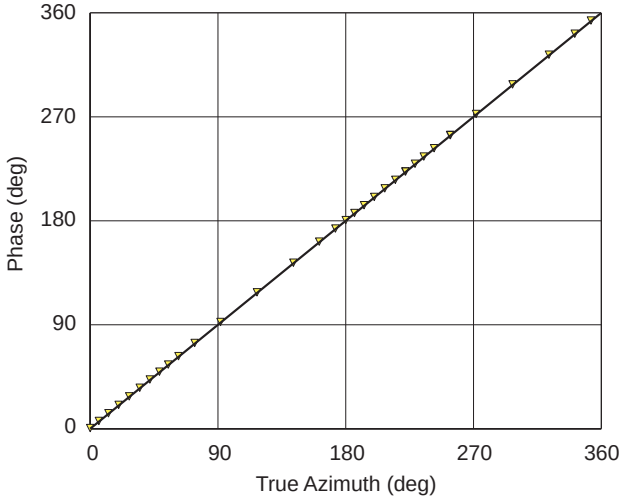

Fig. 9. Calculated phase angle versus true azimuth mass center.

Based on Figs. 7 and 8, it should be possible to correct the balance sensitivity coefficient measured for a single blade to account for changes in the coefficient due to azimuth spacing; but only if the phase angle of the vibratory response is a true indicator of the distribution of mass between two adjacent blades. When masses are added to the tips of two adjacent blades, one can define an equivalent mass equal to the sum of the two blade tip masses. The azimuth location of the mass center of this equivalent mass is defined by

$$\tan(\phi) = \frac{M_1 \sin(\psi_1) + M_2 \sin(\psi_2)}{M_1 \cos(\psi_1) + M_2 \cos(\psi_2)} \tag{1}$$

For each amplitude of the vertical vibratory responses calculated by RCAS and plotted in Fig. 7, there corresponds a phase angle. That phase angle is plotted against the azimuth location of the equivalent mass center of the tip masses in Fig. 9. This figure shows that the phase angle of the vibratory forces calculated by RCAS deviate only slightly from the azimuth location of the mass center for the equivalent mass. Therefore, the phase angle of the vibratory response can be used as an accurate means for distributing mass between two adjacent blade tips.

3.3. Impact on tail rotor balancing operations

In order to assess the impact of the observations above on balancing operations, two hypothetical cases of tail rotor vibration will be simulated using the RCAS tail rotor model. In the first case, it is presumed that the measured vertical vibratory force amplitude is 98.8 lbf, and the measured phase angle is 35.5°. For the second case, the measured amplitude is 56.7 lbf, and the measured phase angle is 92.5°.

To calculate the amount of balance mass required, the amplitude of the vibratory force is divided by the balance sensitivity coefficient (6.9417 lbf/g). Then, that mass is divided between the two blades adjacent to the phase angle of the vibratory force. The amount of mass allocated to each blade is determined by solving Eqs. (1) and (2) simultaneously:

$$m = M_1 + M_2 \tag{2}$$

In the first case, the phase angle of 35.5° indicates that the excess mass is distributed between outboard blade 1 (at 0° azimuth) and inboard blade 1 (at 55° azimuth). The solution to Eqs. (1) and (2) predicts that there is 5.2 g of excess mass at the tip of outboard blade 1 and 9.1 g of excess mass at the tip of inboard blade 1. In fact, the vibratory forces calculated by the RCAS model resulted from placing 6 g at the tip of outboard blade 1 and 10 g of at the tip of inboard blade 1. On an actual blade, mass is added in increments of 2 g, so the rounded values would have resulted in removing exactly the correct amount of mass from each blade. The predictions of the balance masses required were slightly smaller than the actual masses, but were still accurate enough to permit the vibrations to be eliminated on the first iteration.

The 92.5° phase angle calculated by the RCAS model in the second case indicates that the excess mass is distributed between inboard blade 1 (at 55° azimuth) and outboard blade 2 (at 180° azimuth). The predictions from Eqs. (1) and (2) indicate that inboard blade 1 has 5.1 g of excess mass and outboard blade 2 has 3.1 g of excess mass. Again, rounding to the nearest 2 g, 6 g would be removed from inboard blade 1 and 4 g would be removed from outboard blade 2. In this case, the amount of mass added to the blades in the RCAS model was 10 g at the tip of inboard blade 1, and 6 g at the tip of outboard blade 2. Consequently, after the correction was made by removing 6 g from inboard blade 1 and 4 g from outboard blade 2, there still exists an excess of 4 g on inboard blade 1 and 2 g on outboard blade 2. Clearly, the prediction method was not sufficiently accurate to identify the proper amount of mass to be removed.

4. Simple analytical tail rotor model

Using the Rotorcraft Comprehensive Analysis System (RCAS) to simulate the response of the AH-64 tail rotor was useful for obtaining important insights into the behavior of an unbalanced tail rotor. However, there were some limitations to what could be accomplished with that model. First, it would have been difficult and time-consuming to add or remove mass from an arbitrary radial location on any of the blades. Second, while it was easy to calculate the vertical force for the tail rotor hub mounted on a rigid support, calculating the actual vibration levels at the accelerometer location on the vertical tail would be very difficult without a detailed model of the tail boom, vertical tail, and tail rotor hub. In addition, making modifications and running the RCAS model for each case required during the development of improvements to the current balancing procedures would have proven to be exceedingly cumbersome.

4.1. Generic tail rotor

Using the insights gained from the RCAS results shown above, a simple analytical model of a generic tail rotor was developed to assist in further understanding the tail rotor response (see Fig. 10). The blades in the analytical model are assumed to be rigid with no teetering motion, since the RCAS simulations showed that the inner and outer rotors did not exhibit any teetering motion. Mass may be added or removed at any radial location on any blade, or combination of blades. In addition, the azimuthal placement of the blades may be arbitrary. The blades rotate at a constant angular velocity, so the only model degree of freedom is vertical hub motion. Based on the results from RCAS simulations, as reported in [17], aerodynamics and the separation between the two rotors had a minimal effect on the vibratory response. Therefore, both were neglected in this analytical model.

The equation of motion for the unbalanced rotor is shown in Eq. (3). On the right-hand side of the equation is the forcing function that results from mass defects, which in turn causes the vibratory response. Note that the units of Eq. (3) are force:

$$\left[M+\sum_{k=1}^{b}\left(\sum_{j=1}^{N_k} m_{kj}\right)\right]\ddot{z}=\Omega^2 R\sum_{k=1}^{b}\left(\sum_{j=1}^{N_k} m_{kj}\bar{r}_{kj}\right)\cos(\Omega t+\psi_k) \tag{3}$$

For the analytical model to be considered an accurate representation of the RCAS model, the vibratory forces generated by placing defect masses at the tips of adjacent blades should be identical to the vibratory forces calculated by RCAS. A comparison of forces generated by the analytical model with the results shown in Fig. 7 verified that both models yielded identical forces. Therefore, the analytical model will, from this point forward, be used in the same manner as the RCAS model to further investigate the dynamic balance issue.

In order to return a rotor with mass defects to dynamic balance, an additional force, which cancels out the force caused by the mass defects, must be added to the right-hand side of Eq. (3). Let us assume, for the time being, that this force can be generated by placing a mass, m, on the rotor radius at azimuth angle ϕ. Eq. (4) is the equation of motion that results from

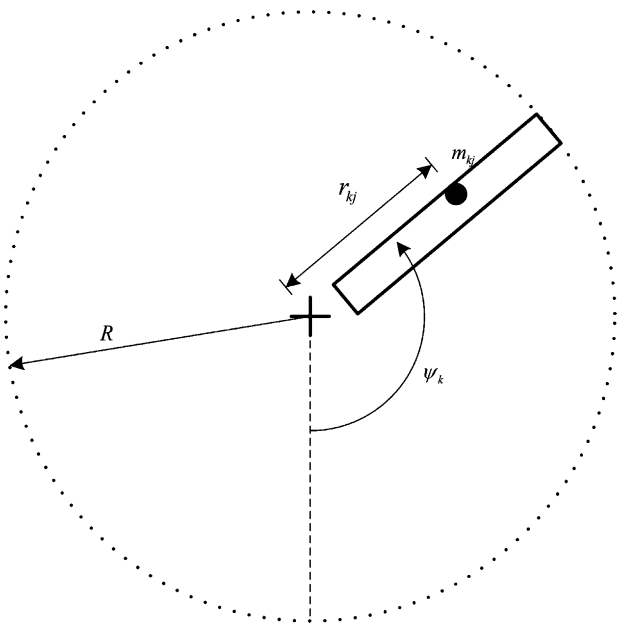

Fig. 10. Analytical tail rotor model.

the equivalent balance mass being added to the rotor:

$$\left[M+m+\sum_{k=1}^{b}\left(\sum_{j=1}^{N_k} m_{kj}\right)\right]\ddot{z} = \Omega^2 R\sum_{k=1}^{b}\left(\sum_{j=1}^{N_k} m_{kj}\bar{r}_{kj}\right)\cos(\Omega t+\psi_k) + \Omega^2 mR\cos(\Omega t+\phi) \tag{4}$$

Since it is common practice to express vibration levels in units of inches per second (ips), rather than in units of force or acceleration, Eq. (4) can be reformulated such that the units are ips. This is accomplished by dividing both sides of the equation by the total mass of the rotor and the rotor speed:

$$\frac{\ddot{z}}{\Omega} = \frac{\Omega R}{M_{\text{total}}}\left[\sum_{k=1}^{b}\left(\sum_{j=1}^{N_k} m_{kj}\bar{r}_{kj}\right)\cos(\Omega t+\psi_k) + m\cos(\Omega t+\phi)\right] \tag{5}$$

where

$$M_{\text{total}} = \left[M+m+\sum_{k=1}^{b}\left(\sum_{j=1}^{N_k} m_{kj}\right)\right] \tag{6}$$

In addition, the quantity that multiplies the right-hand side of Eq. (5) has units of ips/g, which are the same units as the balance sensitivity coefficients that are used in balancing operations. Then, Eq. (4) may be expressed as

$$\frac{\ddot{z}}{\Omega} = C\left[\sum_{k=1}^{b}\left(\sum_{j=1}^{N_k} m_{kj}\bar{r}_{kj}\right)\cos(\Omega t+\psi_k) + m\cos(\Omega t+\phi)\right] \tag{7}$$

where

$$C = \frac{\Omega R}{M_{\text{total}}} \tag{8}$$

In order for the rotor to be in dynamic balance, the sum of the vibrations on the right-hand side of Eq. (7) must be zero. The balance mass, m, and the azimuth angle, ϕ, can be obtained by enforcing the fact that the coefficients of both $\sin\Omega t$ and $\cos\Omega t$ must be zero (harmonic balance):

$$m = \sqrt{\left[\sum_{k=1}^{b}\left(\sum_{j=1}^{N_k} m_{kj}\bar{r}_{kj}\right)\cos\psi_k\right]^2 + \left[\sum_{k=1}^{b}\left(\sum_{j=1}^{N_k} m_{kj}\bar{r}_{kj}\right)\sin\psi_k\right]^2} \tag{9}$$

$$\tan\phi = \frac{\sum_{k=1}^{b}\left(\sum_{j=1}^{N_k} m_{kj}\bar{r}_{kj}\right)\sin\psi_k}{\sum_{k=1}^{b}\left(\sum_{j=1}^{N_k} m_{kj}\bar{r}_{kj}\right)\cos\psi_k} \tag{10}$$

Obviously, it is not possible to place the balance mass at any azimuth location, since the tail rotor has a finite number of blades, and balance masses can only be placed at the tip of a blade. Therefore, unless the azimuth angle, ϕ, is equal to the azimuth offset of one of the blades, balance must be achieved by dividing the mass between the two blades that are adjacent to azimuth angle, ϕ. The problem then is to determine how much mass must be allocated to each blade in order that a force equivalent to the force generated by the single balance mass, m, is obtained.

The two blades between which the mass will be split have azimuth offsets of ψ_R and ψ_L, where $\psi_R \le \phi \le \psi_L$. The balance masses corresponding to each blade are M_R and M_L. The values of the two balance masses are obtained by solving Eq. (11) by harmonic balance:

$$m\cos(\Omega t+\phi) + M_R\cos(\Omega t+\psi_R) + M_L\cos(\Omega t+\psi_L) = 0 \tag{11}$$

Therefore, the required balance masses on the two adjacent blades are

$$M_R = -m\frac{\sin(\psi_L-\phi)}{\sin(\psi_L-\psi_R)} \tag{12}$$

and

$$M_L = -m\frac{\sin(\phi-\psi_R)}{\sin(\psi_L-\psi_R)} \tag{13}$$

Eqs. (12) and (13) will yield result identical to the results that would be obtained from the RCAS model, given identical mass defects. However, neither result is particularly useful for an actual aircraft because the effect of the impedance of the aircraft structure is not modeled. What is needed is a way to include the impedance of the aircraft structure, yet retain the simplicity of the analytical model.

4.2. Apache tail rotor

In the analysis of the preceding section, two assumptions were implicitly made. First, it was assumed that the vibration induced by an unbalanced blade would have the same phase as the blade azimuth angle. That is, if the reference blade is out of balance, the phase of the resulting vibration is 0°. This assumes that the impedance of the structure on which the rotor is mounted must be infinite, which it obviously is not. Measurements taken for the purpose of identifying the balance sensitivity coefficients show that there is a phase difference between an unbalanced blade and the measured vibration. Second, it was assumed that the balance coefficients were the same for all of the blades. While this is true for many rotors, the Apache tail rotor is really two, independent tail rotors. Unique balance sensitivity coefficients and phase angles have been measured for the inner rotor and the outer rotor on the Apache.

Since the Apache tail rotor has unique balance sensitivity coefficients and phase angles for the inner and outer rotors, Eq. (3) must be modified. The modifications account for the fact that a mass defect on an outer rotor blade will result in a different vibration level as compared to a mass defect on an inner rotor blade. Using the balance sensitivity coefficient definition adapted from Eq. (8), the resulting equation of motion is

$$\frac{\ddot{z}}{\Omega} = \sum_{k=1}^{b} C_k \left(\sum_{j=1}^{N_k} m_{kj} \bar{r}_{kj} \right) \cos(\Omega t + \psi_k + \Phi_k) \tag{14}$$

The right-hand side of Eq. (14) can be reformulated into a simple expression that expresses the vibration due to the sum of all mass defects in terms of a single vibration amplitude and a phase angle,

$$\frac{\ddot{z}}{\Omega} = A \cos(\Omega t + \Phi) \tag{15}$$

where

$$A = \sqrt{\left[\sum_{k=1}^{b} C_k \left(\sum_{j=1}^{N_k} m_{kj} \bar{r}_{kj} \right) \cos \Psi_k \right]^2 + \left[\sum_{k=1}^{b} C_k \left(\sum_{j=1}^{N_k} m_{kj} \bar{r}_{kj} \right) \sin \Psi_k \right]^2} \tag{16}$$

and

$$\tan \Phi = \frac{\sum_{k=1}^{b} C_k (\sum_{j=1}^{N_k} m_{kj} \bar{r}_{kj}) \sin \Psi_k}{\sum_{k=1}^{b} C_k (\sum_{j=1}^{N_k} m_{kj} \bar{r}_{kj}) \cos \Psi_k} \tag{17}$$

where

$$\Psi_k = \psi_k + \Phi_k \tag{18}$$

As in the analysis performed in the previous section, mass must be added to (or subtracted from) the rotor at a resultant azimuth angle of Φ in order to cancel out the vibration due to the mass defects. In this case, however, the adjacent blades cannot be determined only on the basis of their azimuth location. The balance phase angles of each blade must also be considered. Therefore, the adjacent blades must satisfy a relationship defined by $\Psi_R \le \Phi \le \Psi_L$.

In order to balance the rotor, mass is added to, or removed from, the adjacent blades. The modified equation of motion for the rotor is then obtained by adding the additional mass terms to Eq. (15):

$$\frac{\ddot{z}}{\Omega} = A \cos(\Omega t + \Phi) + C_R M_R \cos(\Omega t + \Psi_R) + C_L M_L \cos(\Omega t + \Psi_L) \tag{19}$$

The solution for the mass to be added to, or removed from, each of the adjacent blades is found by setting the left-hand side of Eq. (19) to zero and using harmonic balance to solve for M_R and M_L:

$$M_R = -\frac{A \sin(\Psi_L - \Phi)}{C_R \sin(\Psi_L - \Psi_R)} \tag{20}$$

$$M_L = -\frac{A \sin(\Phi - \Psi_R)}{C_L \sin(\Psi_L - \Psi_R)} \tag{21}$$

The expressions for M_R and M_L in Eqs. (20) and (21) are analogous to Eqs. (12) and (13). The difference is that the former equations account for the fact that the inner and outer rotors have a different balance coefficient and balance phase angle. By using the measured balance sensitivity coefficients and phase angles, this model has incorporated the effect of structural impedance without the need for a complex structural model of the aircraft.

5. Apache tail rotor balance calculations

The principal objective of this investigation is to improve the accuracy and efficiency of the methods used to balance the Apache tail rotor. As described above, when the mass of more than one blade is different from that of a nominal blade, balance coefficients used in the conventional manner may be quite inaccurate and/or inefficient. There are three possible solutions to improve the balance coefficients: (1) measure balance coefficients, varying the amount of mass on each blade in a manner similar to the RCAS simulations; (2) calculate balance coefficients from an analytical model, such as RCAS; or (3) develop a means to correct the existing balance coefficients such that they become functions of the measured phase angle. The first alternative is impractical because of the large number of data collection flights that would be required to collect the vibration data. In order to get the same phase resolution as that obtained from the RCAS simulations, 15 times as many flights would be required as compared to measuring a single balance coefficient. Alternative (2) is also impractical because the fidelity required from an analytical simulation would be very difficult, if not impossible, to attain. That leaves the third alternative as the most practical.

In order to test the algorithm described above, two scripts were written using the Python computer language. One script (`calcVibs`) calculates the amplitude and phase of the vertical vibration resulting from a set of mass defects in the rotor blades, using Eqs. (16) and (17). The other script (`balanceTR`) calculates the exact amount of mass that must be added to the blade tips in order to drive the vibration to zero, given the amplitude and phase of the vertical vibration. Since the vibration phase angle, Φ, always indicates the "heavy" rotor azimuth, the algorithm always suggests removing mass from the blades adjacent to Φ. However, three other solutions are possible. For example, assume that the algorithm suggests removing M_R from the blade at ψ_R and removing M_L from the blade at ψ_L. An equally valid solution could be obtained by adding M_L to the blade at $\psi_L + 180^\circ$, or by adding M_R to the blade at $\psi_R + 180^\circ$, or both. These optional solutions are equally accurate, and may prove necessary if there are no tip masses to remove on one or more of the affected blades.

To show the qualitative difference that the structural impedance makes in the response of the rotor to mass defects, Fig. 11 shows the vibratory response at the accelerometer location on the vertical tail due to rotor imbalance. This figure was created using the analytical model of the Apache rotor and the balance sensitivity coefficients and phase angles measured on the AH-64D tail rotor. The plotted points were generated by `calcVibs` using the same method that was used to create Figs. 7 and 8, where 16 g of mass were transferred in 2 g increments from blade to blade, until mass imbalance traversed the entire azimuth of the rotor. One of the primary differences between Figs. 7 and 11 is that in Fig. 7, the azimuth location of each blade corresponds to the phase angle of the four response peaks. In Fig. 11, however, this relationship is altered because of the measured phase shift of 160° for the outer blades and 166° for the inner blades. In addition, Fig. 7 shows that the maximum amplitudes of the forces that result from the mass imbalance are equal for all four blades. On the other hand, Fig. 11 shows that the maximum amplitudes of the vibrations differ for the outer and inner rotor blades. This occurs because the measured sensitivity coefficients for the outer and inner rotor blades are not equal. That is, a mass imbalance in the outer rotor results in more vibratory response than the same imbalance in the inner rotor would produce.

In order to test `balanceTR`, the script that calculates the amount of tip mass that must be removed from the blade tips in order to eliminate the vibratory response, several simple cases were run. First, all of the imbalance cases in Fig. 11 were tested; and in each case, the solution produced by the algorithm correctly identified the heavy blades, and suggested removing the precise amount of mass that had been added to each blade. Next, the converse of Fig. 11 cases were run by removing mass from the blades. In these cases, the solutions identified the blades on the opposite side of the rotor as being the heavy blades, and suggested removing the precise amount of mass from each that was originally removed from the opposite blades. Finally, a number of test cases were run to test the ability of `balanceTR` to produce a balance solution that completely eliminated the vibration response. A selected few of those cases are shown in Table 1. The procedure used was

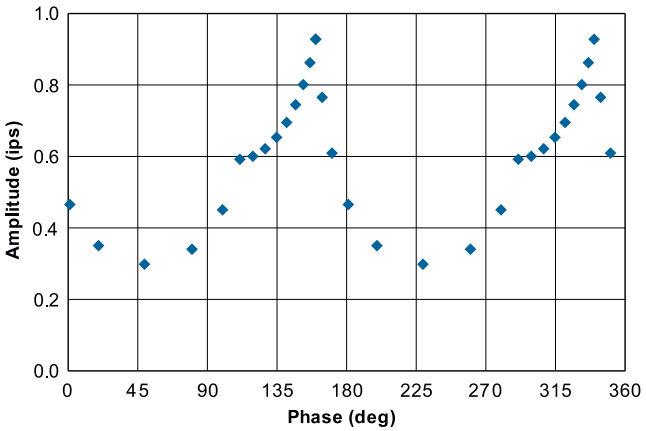

Fig. 11. Vertical vibration versus phase angle for 16 g total mass.

Table 1
Selected test cases used for validation.

Case	Defects			Balance solution	
	Blade	Mass (g)	Radius	Blade	Mass (g)
1	OB1	16	0.5	OB1	−8.0
2	OB1	16	0.5	OB2	8.0
	IB1	−16	1.0	IB1	16.0
3	OB1	16	0.5	OB1	−10.25
	IB1	8	1.0	IB1	−8.0
	OB2	−3	0.75		
4	OB1	16	0.5	OB1	−10.25
	IB1	8	1.0	IB1	−9.25
	OB2	−3	0.75		
	IB1	5	0.25		

Table 2
Balance solutions for AH-64D tail rotor imbalance.

Case	Defect vibration		Balance solution		Residual vibration	
	Amplitude (ips)	Phase (deg)	Blade	Mass (g)	Amplitude (ips)	Phase (deg)
1	0.22	202	OB1	−6	0.04	7.6
			IB2	−6		
2	0.41	14	OB2	−10	0.05	152.7
			IB1	−8		
3	0.67	326	OB2	−8	0.04	−12.3
			IB2	−6		
4	1.38	97	OB2	−8	0.02	157.6
			IB1	−44		

to first calculate the vibration response due to the mass defects (shown on the left-hand side of Table 1) with `calcVibs`. That response was then used as input to `balanceTR`, which calculated the response solution (shown on the right-hand side of Table 1). Finally, `calcVibs` was used to calculate the vibration response due to the combination of the mass defects and the balance solution. In every case tested, the amplitude of the vibratory response was zero.

It has been shown that `calcVibs` is capable of calculating the vibratory response for a complex set of mass defects; and that `balanceTR` is capable of finding a balance solution that will eliminate the vibratory response. However, in practice, the specific mass defects are unknown, and only the vibratory amplitude and phase are known from accelerometer measurements. Furthermore, on the AH-64D, mass may only be added or removed from the blade tips in 2 g increments. As a result, Cases 3 and 4 in Table 1 do not represent realistic balance solutions. Therefore, an additional set of test cases were run, where only the vibration amplitude and phase were given. For these cases, `balanceTR` calculated the precise amount of tip mass required on each blade, and those values were rounded to the nearest 2 g. Then, `calcVibs` calculated the vibratory amplitude and phase of the balance solution vibratory response independent of the response due to mass defects. The vector sum of the vibratory response due to the rotor imbalance and the independent vibratory response from the balance solution constitutes the residual vibration after the balance correction. Table 2 shows sample results for four cases in which the vibration amplitudes range in value from typical to high for the AH-64D, and phase angles which were chosen at random. Note that in all cases, the balance solution reduced the residual vibratory amplitude to an acceptable level (<0.15 ips) in a single step.

6. Conclusions

Results from the simulations performed with the RCAS model of the Apache tail rotor showed that difficulties in balancing certain Apache tail rotors most likely occur when balancing requires that mass must be added to or removed from two adjacent blades, particularly blades that are separated by 125°. The problem is that the relationship between the

amplitude of the vibratory response and the tip mass, which determines the balance sensitivity coefficient, depends on the phase angle of the vibratory response. This dependency is particularly evident as the azimuth separation between blades becomes larger. The effect is not nearly as significant when the separation is small. Therefore, balancing tail rotors where mass must be added to or removed from blades that are separated by 125° may be problematic.

A simplified, analytical model of a generic tail rotor was developed in order to overcome some of the restrictions and inconveniences of using the RCAS model. With this model, it is possible to define a general set of mass defects and compute the resulting 1/rev vibration response, if the influence of structural impedance is known. It was shown that the effect of structural impedance can be represented by the balance sensitivity coefficient. This coefficient is known for most rotors, since it is currently measured and used in conventional, rotor balancing algorithms. Therefore, the generic model must be specialized in order to be useful for balancing a specific rotor.

The simple, generic, analytical tail rotor model was modified to address specific characteristics of the Apache tail rotor, including the difference in balance sensitivity coefficients and phase angles between the outer and inner rotor blades. Through the use of the measured coefficients and phase angles, the modified analytical model could account for the effect of the impedance of the tail structure on the accelerometer readings. Algorithms based on the model were developed to compute the vibratory response due to a set of mass defects, and to compute the amount of tip mass required on each blade to eliminate a given level of 1/rev vibration. Sample calculations for the AH-64D tail rotor showed that the balance algorithm is very effective in reducing vibrations to an acceptable level. While these tests demonstrate that this methodology has the potential for improving rotor balancing operations, conclusive proof of its practicality can only be determined by similar tests performed on actual aircraft.

References

[1] P. Jackson, *Jane's All the World's Aircraft*, Cambridge University Press, Great Britain, 2001–2002, 2006–2007.
[2] V. Giurgiutiu, G. Craciun, A. Rekers, Cost benefit analysis models for evaluation of VMEP/HUMS project, in *Proceedings of the 55th Meeting of the Society for Machinery Failure Prevention Technology*, Virginia Beach, VA, April 2001.
[3] A. Rosen, R. Ben-Ari, Mathematical modelling of a helicopter rotor track and balance: theory, *Journal of Sound and Vibration* 200 (5) (1997) 589–603.
[4] R. Ben-Ari, A. Rosen, Mathematical modelling of a helicopter rotor track and balance: results, *Journal of Sound and Vibration* 200 (5) (1997) 605–620.
[5] E. Bechhoefer, D. Power, IMD HUMS rotor track and balance techniques, in *IEEE Aerospace Conference Proceedings, No. IEEEAC 1191*, Big Sky, Montana, March 2003.
[6] S. Wang, K. Danai, M. Wilson, A probability-based approach to helicopter rotor tuning, *Journal of the American Helicopter Society* 50 (1) (2005) 56–64.
[7] H.J. Taitel, K. Danai, D. Gauthier, Helicopter track and balance with artificial neural nets, *ASME Journal of Dynamic Systems, Measurement, and Control* 117 (2) (1995) 226–231.
[8] D. Wroblewski, P. Grabill, J.D. Berry, R.W. Branhof, Neural network system for helicopter rotor smoothing, in *IEEE 2000 Aerospace Conference*, Big Sky, Montana, March 2000, pp. 271–276.
[9] D. Wroblewski, R.W. Branhof, T. Cook, Neural networks for smoothing of helicopter rotors, in *American Helicopter Society 57th Annual Forum Proceedings*, Washington, DC, May 2001, pp. 1587–1594.
[10] R.R.K. Reddy, R. Ganguli, Structural damage detection in a helicopter rotor blade using radial basis function neural networks, *Smart Materials & Structures* 12 (2) (2003) 232–241.
[11] R. Ganguli, I. Chopra, D.J. Haas, Helicopter rotor system fault detection using physics-based model and neural networks, *AIAA Journal* 36 (6) (1998) 1078–1086.
[12] R. Ganguli, Health monitoring of a helicopter rotor in forward flight using fuzzy logic, *AIAA Journal* 40 (12) (2002) 2373–2382.
[13] D. Yang, S. Wang, K. Danai, Helicopter track and balance by interval modeling, in *Proceedings of the 57th American Helicopter Society Annual Forum*, Washington, DC, May 2001, pp. 1577–1586.
[14] H.E. Jones, D.L. Kunz, Comprehensive modeling of the Apache in CAMRAD II, in *Proceedings of the AHS International Structures Specialists' Meeting*, Williamsburg, VA, October 2001.
[15] N.A. Miller, D.L. Kunz, A comparison of main rotor smoothing adjustments using linear and neural network algorithms, *Journal of Sound and Vibration* 311 (3–5) (2008) 991–1003.
[16] Headquarters, Department of the Army, Operator's, Aviation Unit, and Intermediate Maintenance Manual Including Repair Parts and Special Tools List for Test Set, Aviation Vibration Analyzer (AVA), Version 7.01 Edition, TM 1-6625-724-13&P, Mar 2002.
[17] M.A. Newkirk, Process Improvements for the AH-64 Tail Rotor Vibration Analysis, Master's Thesis, Air Force Institute of Technology, Wright-Patterson AFB, OH, AFIT/GAE/ENY/07-J15, June 2007.